

# 3D Localization Technique for Broad Band Impulsive Noise Source

Nur Ibrahim<sup>1</sup>, Irma Safitri<sup>1</sup>, Efrina Yanti Hamid<sup>2</sup>, and Redy Mardiana<sup>3</sup>

<sup>1</sup>School of Electrical Engineering, Telkom University, Bandung, Indonesia

<sup>2</sup>School of Electrical Engineering, Institut Teknologi Bandung, Jl. Ganesa 10, Bandung, Indonesia

<sup>3</sup>Department of Electrical Engineering, The Petroleum Institute, Umm Al Naar, Abu Dhabi, United Arab Emirates  
(Tel : +62-812-202-6833; E-mail: nuribrahim.nib@gmail.id)

**Abstract**—This paper presents a three-dimensional (3D) localization system for locating partial discharge (PD) on high-voltage apparatuses. An antenna array consisted of four sensors is employed to record the electromagnetic waves (EM) emitted from PD. The localization algorithm is based on the time difference of arrival (TDOA) of the signals. The TDOAs can be determined using the cross-correlation method, peak detection method, Akaike Information Criterion (AIC) method, Energy Criterion (EC) method, Gabor Centroid method, and/or threshold detection method. These system use two kind of antenna configurations. The first configuration is squared array with distance between antennas are 2 meter, and the second configuration is squared array with distance between antennas are 4 meter. In experimental setup, the implemented configuration is the first configuration, due to limitation of the experiment area. The effectiveness of the location method is tested through a computer simulation and the results are presented. From simulation result, the second configuration gives 11.12% better accuracy than the first configuration.

**Keyword:** impulsive noise, PD, antennas array, TDOA, 3D Localization.

## I. INTRODUCTION

In recent years, there has been an increasing concern about the interference of impulsive noise with communication systems, such as wireless communications, television and radio broadcasts, and so forth. Among others, more attention is paid to the electromagnetic (EM) interference from partial discharges (PD) from high voltage apparatuses (e.g. outdoor insulators of power lines). PD due to the defects in the power apparatus may serve as successive noise sources for an entire neighborhood continuously, while noises occurring in vehicle ignition systems, microwave ovens, and so forth are temporary. The frequency spectra of impulsive noise from power lines are mostly within the order of tens to hundreds of megahertz. This covers the frequency bands of broadcasters.

For a better EM environment, it is desirable to find the location of the impulsive noise sources. This enables us to take appropriate actions in order to remove the noise source. The technique to locate the EM noises due the electrical discharges was described over 40 years ago [1] using the measurements of traveling electromagnetic phenomena. Subsequently, many studies have introduced the noise source location techniques with better accuracy and sensitivity [2–4].

There has been relatively little progress on a locating

system that can be generally applied in a substation environment, rather than specifically applied to an item in the power plant. In this context, the use of radio frequency remote sensing holds the biggest promise since it can be easily deployed in a substation, does not require any physical contact, and can be applied to any energized power plant.

The 3D location techniques to locate noise source have well documented. Challa and Shamsunder [6] proposed a high-resolution subspace approach for localizing near field EM sources in three-dimensional spaces. They validated their proposal numerically. This approach is, however, limited to the localization of narrow-band sources. Peck and Moore [7] demonstrated the adoption of the HT algorithm [5] for TDOA estimation. This resulted in an improved performance of the direction-of-arrival (DOA) estimation. It should be noted that previous papers on this estimation for noise sources were mostly concentrated on measurement, together with simple theory. In a theoretical model, a plane wave is considered as the wave source.

In this paper, we attempt to estimate the 3D locations of noise sources from PD occurred in a substation using an antenna array. The localization algorithm is based on the time difference of arrivals (TDOAs) of noise sources which are received by spatially separated antennas. The TDOAs can be determined using the cross-correlation method [5], peak detection method, Akaike Information Criterion (AIC) method, Energy Criterion (EC) method, Gabor Centroid method, and/or threshold detection method. The performance of the technique is evaluated quantitatively through a numerical simulation.

## II. 3D LOCALIZATION METHOD

### A. Basic Principle

At least four antennas are required for the 3D localization of the noise source. The geometry of antenna configuration is illustrated in Figure 1. The antennas are arranged at the vertices of a square with a base line's length  $d$ . The location of the noise source  $P$  is assumed to be as unknown variables  $(x, y, z)$ . The four antennas are labeled 1, 2, 3, and 4, and their co-ordinates are  $(x_1, y_1, 1)$ ,  $(x_2, y_2, 1)$ ,  $(x_3, y_3, 1)$ , and  $(x_4, y_4, 1)$  meters, respectively. It should be noted that three independent values of TDOAs can be obtained from these four antennas configuration. The signal received by antenna 1 is chosen as the reference signal. The relations between the

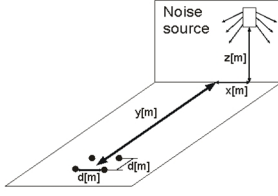


Fig. 1. Geometry of 3D location method.

coordinates of the antennas and TDOAs are represented by the following non-linear equation:

$$c\Delta t_{12} = \sqrt{(x-x_2)^2 + (y-y_2)^2 + (z-z_2)^2} - \sqrt{(x-x_1)^2 + (y-y_1)^2 + (z-z_1)^2} \quad (1)$$

$$c\Delta t_{13} = \sqrt{(x-x_3)^2 + (y-y_3)^2 + (z-z_3)^2} - \sqrt{(x-x_1)^2 + (y-y_1)^2 + (z-z_1)^2} \quad (2)$$

$$c\Delta t_{14} = \sqrt{(x-x_4)^2 + (y-y_4)^2 + (z-z_4)^2} - \sqrt{(x-x_1)^2 + (y-y_1)^2 + (z-z_1)^2} \quad (3)$$

where  $\Delta t_{ij}$  denotes the TDOA between antenna  $i$  and  $j$ , and  $c$  is the speed of electromagnetic wave in free space ( $c = 3 \times 10^8$  m/s). The location of the noise source  $P(x, y, z)$  can be estimated if a set of TDOAs values are obtained. The solution the non-linear equation above can be obtained using the well-known Newton-Raphson iteration technique.

### B. Discharge source model

The impulsive noise source signal from a partial discharge is modeled by a multiplication of sinusoidal signal and double-exponential form defined the following equation:

$$S(t) = A_0 \sin(2\pi ft) \left( -\exp\left(-\frac{t}{\tau_1}\right) + \exp\left(-\frac{t}{\tau_2}\right) \right) \quad (4)$$

Parameters of discharge source model is:

$A_0$	$\tau_1$ (ns)	$\tau_2$ (ns)	$c$ (m/s)	$f$ (MHz)
2.6	40	50	$3 \times 10^8$	50

Fig. 2 shows the source signal model for a period of 1 micro second, as suggested in [10]. In the simulation, a Gaussian noise with a signal-to-noise ratio (SNR) of 10 dB is added to the discharge source model in order to complicate the analysis of 3D source location, based on [11].

### C. Estimation of TDOA

#### Cross-Correlation Method

A signal received at two spatially separated antennas can be mathematically modeled as

$$s_1(t) = S(t) + n_1(t) \quad (5)$$

$$s_2(t) = \alpha S(t - \Delta t_{21}) + n_2(t) \quad (6)$$

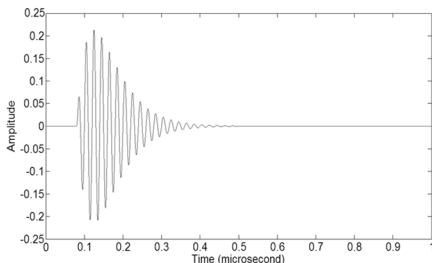


Fig. 2. The waveform of the discharge source model.

where  $S(t)$  is the original impulsive source signal,  $n_1(t)$  and  $n_2(t)$  are additive noise sources which are uncorrelated and have zero mean values,  $\alpha$  is an attenuation factor, and  $\Delta t_{21}$  is the TDOA between the received signals. A measure of similarity between a pair of energy signals,  $s_1(t)$  and  $s_2(t)$ , can be defined through the cross-correlation sequence  $r_{s_1 s_2}(\Delta t)$ , defined by the following equation:

$$r_{s_1 s_2}(\Delta t) = \int_{-\infty}^{\infty} s_1(t) s_2(t - \Delta t_{21}) d\Delta t \quad (7)$$

The  $\Delta t$  is called the time-lag and indicates the time-shift between the signal pair. This cross-correlation method is utilized to estimate time delay by detecting the time that maximizes its function. The time-lag that gives maximum value of the cross-correlation function is the estimated TDOA.

#### Peak Detection Method

This method is used to predict time of arrival (TOA) by detect the time of received signal that have maximum value, from each antenna. So, we obtained four TOA value from four antennas.

By using first antenna as reference antenna, TDOAs can be obtained by the following equation:

$$\text{TDOA}_{12} = \text{TOA}_2 - \text{TOA}_1 \quad (8)$$

$$\text{TDOA}_{13} = \text{TOA}_3 - \text{TOA}_1 \quad (9)$$

$$\text{TDOA}_{14} = \text{TOA}_4 - \text{TOA}_1 \quad (10)$$

#### Akaike Information Criterion (AIC) Method

AIC is a measure of the goodness of fit of a statistical model to a set of observations. It can be used to estimate TOA of PD pulses that received at each antenna.

This method defines the curve  $\text{AIC}_k$  as:

$$\text{AIC}_K = k \cdot \ln(\sigma_{1,k}^2) + (N - k - 1) \cdot \ln(\sigma_{k+1,N}^2) \quad (11)$$

where  $\sigma_{m,n}^2$  is the variance of signal  $s_k$  (received signal in antennas), where  $k$  is the index from 1 up to  $N$ .  $N$  is amount of signal sample. The value of  $\text{AIC}_K$  is calculated for each sample in the signal  $s_k$ . TOA is the global minimum of all  $\text{AIC}_K$  values. In order to prevent ambiguous results, the signal is cropped so that the pulse onset occurs in the second half of the signal, as suggested in [7].

#### Energy Criterion (EC) Method

This method is based on the energy that contained in the signal. It combines the partial signal energy with a negative trend [6].

The signal  $\text{EC}_K$  is defined by the following equation:

$$\text{EC}_K = \sum_{i=1}^k s_i^2 - k \cdot P_s \quad (12)$$

where  $P_x$  is mean power from  $x_k$ . The value of  $\text{EC}_K$  is calculated for  $k$  ranging from 1 to  $N$ . The global minimum value of  $\text{EC}_K$  are TOA.

#### Gabor Centroid Method

Gabor defines the “epoch” of order 1 of a signal [8]. By assuming that the signal is real, converting it to time-discrete form, and adding two extra terms to remove noise-dependency, this “epoch” is defined by the following equation:

$$\text{TOA}_g = \frac{\sum_{k=1}^N t_k s_k^2 - P_n \sum_{k=1}^N t_k}{\sum_{k=1}^N s_k^2 - P_n \cdot N} \quad (13)$$

where  $t_k$  is the time corresponding to index  $k$ .  $P_n$  is the mean power of  $\eta_k$ .

#### Threshold Detection Method

Threshold detection method defines TOA when signal  $S_k$  exceeds a certain threshold level  $S_{\text{thres}}$ . This is a straightforward method that can easily be implemented. Therefore, this method is used in many PD detection systems.

The threshold level is chosen relative to the noise level, so that it always low as the noise permits without too many false trigger. This is the following equation to determine threshold level:

$$S_{\text{thres}} = m \cdot \sqrt{P_n} \quad (14)$$

where  $m$  is a parameter chosen by the user. In this paper, the value  $m=5$  is used, to avoid Gaussian noise with a signal-to-noise ratio (SNR) of 10 dB that added to the discharge source model (in simulation) and to avoid background noise (in experiment) being calculated when processing received signal.

### III. EXPERIMENTAL SETUP

#### A. Measurement System Configuration

The proposed measuring system employed four broad band antennas. They are separated horizontally with the base line's length  $d$ . The base line's length can be adjusted. The antennas are connected to a Digital Phospor Oscilloscope (DPO) 7254 through  $50 \Omega$  coaxial cables with the length of 8 m each. The impulsive noise signal is digitized at 1 GHz sampling rate using a DPO that having 8-bit resolution. The pre-trigger setup was 30%. The system was operated to record discharge sources up to  $f_c = 500$  MHz (Nyquist frequency). The equipments used in this experiment are:

- Digital Phospor Oscilloscope (DPO) 7254 (Fig. 3)
  - Four (4) monopole antennas
  - Four (4) coaxial cables with the length of 8 m each
  - Four (4) tripods
  - Noise source generator (Fig. 4) which is made from spark plug that powered by 3.7 volt lithium battery
- Then, these equipments are assembled as shown in Fig. 5.

#### B. Configuration System

In the numerical simulation, we use two antenna configurations. The first antenna configuration is a squared



Fig. 3. Digital Phospor Oscilloscope (DPO) 7254



Fig. 4. Noise source generator



Fig. 5. Assembled equipments for noise source detection

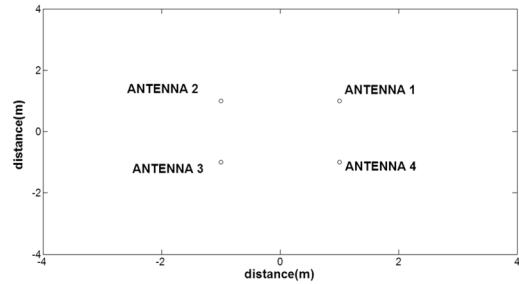


Fig. 6. Squared array configuration with antenna spacing of 2 meters.

array as shown in Fig. 6. The antennas are located 1 meter above the ground.

### IV. SIMULATION & EXPERIMENTAL RESULTS

#### A. Simulation Results

The performance of the proposed technique is evaluated quantitatively through numerical simulation. A total of 100 noisy signals at a given location generated. Two different base line's length are chosen,  $d = 2$  m and  $d = 4$  m. The signal-to-noise ratio is fixed at 10 dB. For the given source location and base line's length, the TDOAs and the source location are estimated.

Fig. 7 shows the time delays of arrivals for the total of 100 samples with base line's length of  $d = 2$  m. The true noise source location is assumed to be located at  $P(10, 10, 1)$  m. The solid horizontal lines are the ideal time difference; meanwhile the dots indicate the estimated time difference. Note that subscripts  $i$  and  $j$  in  $t_{ij}$  means the time delay of arrival between the antennas  $i$  and  $j$ .

Similarly, Fig. 8 shows the time delay of arrivals for the total of 100 samples with base line's length of  $d = 4$  m. As seen from both figure, the errors caused by the measurements

are small and it can be negligible for localization accuracy.

Fig. 9 shows the corresponding results of 3D source localization for the base line's length of  $d = 2$  m. The true noise source location is located at P (10, 10, 1) m. The location of each antenna and the true location of noise source are indicated. Similarly, Fig. 10 shows the result of 3D source localization for the base line's length of  $d = 4$  m.

It is noteworthy that only the calculation results which give convergence solution are plotted. This is because the divergence solution may occur when running the Newton-Raphson iteration method. Such divergences are caused by the significant difference between ideal and measured TDOAs. From the figures, it can be seen that the location error of the proposed method is acceptable.

From Table I, it can be seen that cross-correlation method gives smallest error of distance and smallest standard deviation. Also, from Table I, cross-correlation method with  $d = 4$  m gives 11.12% better accuracy than cross-correlation method with  $d = 2$  m.

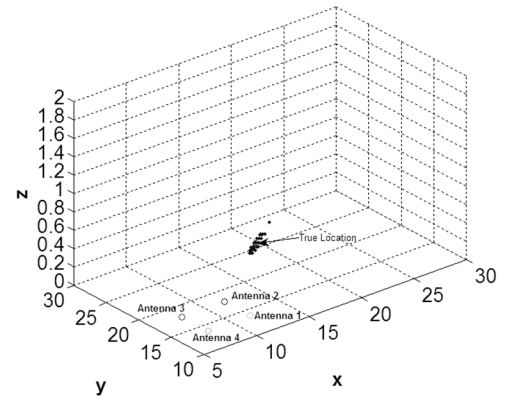


Fig. 10. Simulation result of 3D localization with  $d = 4$  meters.

TABLE I  
COMPARISON BETWEEN SQUARED ARRAY WITH  $d = 2$  m AND SQUARED ARRAY WITH  $d = 4$  m.

Method	Parameter	$d = 2$ m	$d = 4$ m
AIC	ex	24.8823	78.8622
	stdev_ex	56.4865	329.6932
	ey	28.8397	83.3685
	stdev_ey	68.2429	329.2234
	ez	23.7596	40.1662
	stdev_ez	109.2877	203.4344
	er	50.7209	143.7751
EC	stdev_er	131.1244	500.6845
	ex	18.8073	4.0833
	stdev_ex	41.4135	6.9670
	ey	18.8938	3.9919
	stdev_ey	41.4723	6.7049
	ez	0	0
	stdev_ez	0	0
Gabor	er	26.6670	5.7046
	stdev_er	58.5966	9.6623
	ex	34.7943	28.1513
	stdev_ex	68.1542	50.7860
	ey	34.4350	27.9105
	stdev_ey	69.2925	49.7474
	ez	0.0048	0
Peak Detection	stdev_ez	0.0419	0
	er	49.6027	39.7646
	stdev_er	0.1735	1.1996
	ex	23.9864	7.8503
	stdev_ex	39.2486	25.8594
	ey	24.5775	6.4861
	stdev_ey	40.2943	22.3846
50% Peak Detection	ez	0.0002	0
	stdev_ez	0.0023	0
	er	33.6195	9.8227
	stdev_er	50.4421	32.4109
	ex	19.0775	90.2414
	stdev_ex	28.0968	488.1856
50% Peak Detection	ey	15.0164	88.8961
	stdev_ey	26.2856	488.4720
	ez	0	128.3703
	stdev_ez	0	401.0953

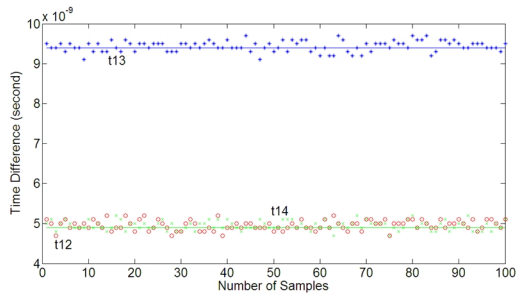


Fig. 7. The time difference between the antennas with  $d = 2$  meters.

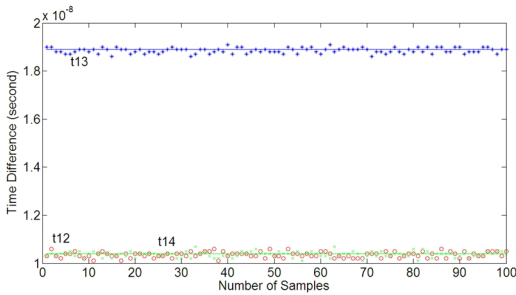


Fig. 8. The time difference between the antennas with  $d = 4$  meters.

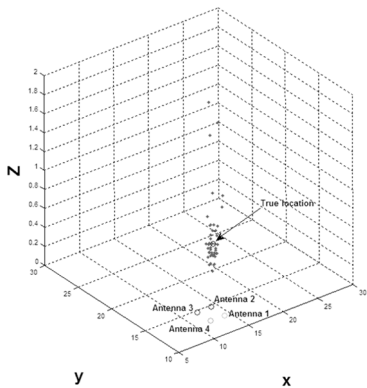


Fig. 9. Simulation result of 3D localization with  $d = 2$  meters.

	er	20.3764	211.4017
	stdev_er	36.1553	778.4429
20% Peak Detection	ex	80.5112	25.6562
	stdev_ex	271.1439	105.0660
	ey	69.7131	23.9045
	stdev_ey	252.0556	96.8719
	ez	0	47.9952
	stdev_ez	0	278.6735
Threshold	er	101.1975	67.8797
	stdev_er	355.0842	305.4884
	ex	13.2098	4.0985
	stdev_ex	24.0423	6.6438
	ey	12.9049	4.0070
	stdev_ey	23.1400	6.4403
Cross-correlation	ez	0.0024	0
	stdev_ez	0.0242	0
	er	18.4714	5.7281
	stdev_er	33.3188	9.2356
	ex	1.5701	0.4266
	stdev_ex	2.9819	0.5403
	ey	1.5609	0.4076
	stdev_ey	2.9712	0.5281
	ez	0	0
	stdev_ez	0	0
	er	2.1611	0.5888
	stdev_er	4.2072	0.7524

Note :

- ex = error of x coordinate (m)
- stdev\_ex = standard deviation of x (m)
- ey = error of y coordinate (m)
- stdev\_ey = standard deviation of y (m)
- ez = error of z coordinate (m)
- stdev\_ez = standard deviation of z (m)
- er = error of distance from (0,0,0) to PD source location (m)
- stdev\_er = standard deviation of r (m)

## B. Experimental Results

In this experiment, two noise source location is used. P1 is the highest location in experiment area, and P2 is the farthest location in experiment area.

Here are the experimental results of detecting the noise source location in the field by using 4 monopole antennas that configured in squared-shape, and put noise source generator which is made from spark plug that powered by 3.7 volt lithium battery.

### 1. Received signal in each antenna

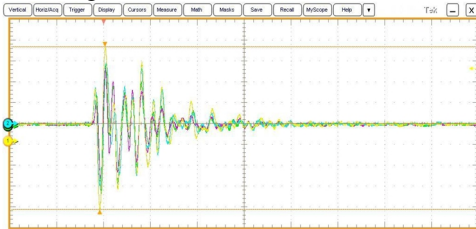


Fig. 11. Noise source signals that captured by each antenna using DPO

Note:

- Red signal is a received signal by antenna 1.
- Green signal is a received signal by antenna 2.
- Yellow signal is a received signal by antenna 3.

- Blue signal is a received signal by antenna 4.
- The signals is sampled at 10 GHz frequency sampling, 2 microsecond along (x-axis), with 1.5 mV/div amplitude (y-axis).

### 2. TDOA

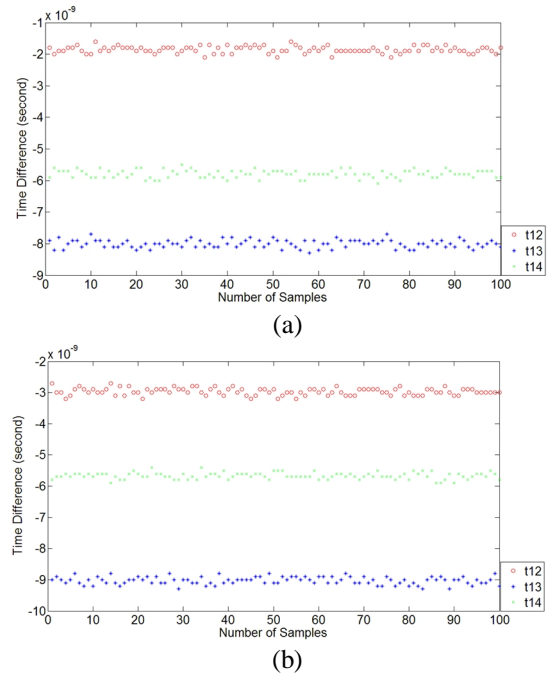


Fig. 12. TDOAs between antennas (antenna 1 as reference antenna), result of calculation using cross-correlation method, for square array configuration, with noise source location (P): (a) P1 = [-3.13, -9.21, 4.22] meter, (b) P2 = [-7.36, -13.72, 0.84] meter

### 3. The result of location estimation of noise source

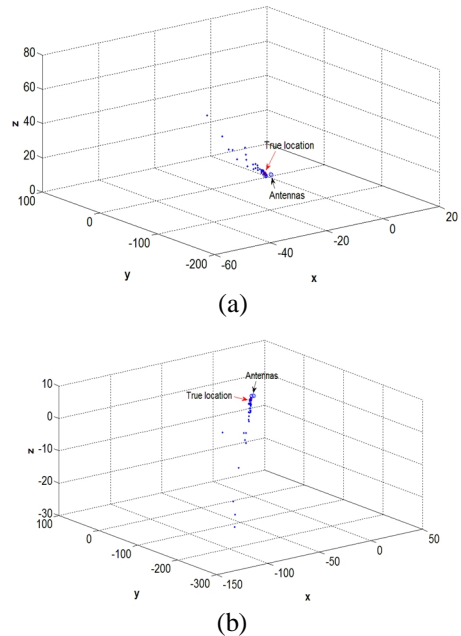


Fig. 13. The result of location estimation of noise source, using cross-correlation method, for square array configuration, with noise source location (P): (a) P = (-3.13, -9.21, 4.22) meter, (b) P = (-7.36, -13.72, 0.84) meter

The following table show the TDOAs ideal value for square array configuration, with the distance between antennas  $d = 2$  m.



## V. CONCLUSION

TABLE II  
TDOAs IDEAL VALUE FOR SQUARED ARRAY CONFIGURATION, WITH NOISE SOURCE COORDINATE P : P1 = [-3.13, -9.21, 4.22] m, P2 = [-7.36, -13.72, 0.84] m

P	t12 (ns)	t13 (ns)	t14 (ns)
P1	-1.86	-8.01	-5.79
P2	-2.98	-9.02	-5.69

TABLE III  
TDOAs MEAN VALUE OF EACH METHODS FOR SQUARED ARRAY CONFIGURATION, WITH NOISE SOURCE COORDINATE P : P1 = [-3.13, -9.21, 4.22] m, P2 = [-7.36, -13.72, 0.84] m

P		P1			P2		
Mean (ns)		t12	t13	t14	t12	t13	t14
Method	AIC	-2.12	-17.13	-11.94	-3.32	-9.81	-6.84
	EC	-1.87	-7.95	-5.74	-2.99	-9.04	-5.73
	Gabor	-2.08	-8.72	-6.29	-3.40	-9.13	-6.11
	peak	-2.18	-8.03	-0.48	-2.95	-7.44	0.17
	50% peak	1.43	-12.11	-7.40	0	-9.05	-3.47
	20% peak	-2.14	-7.44	-1.78	-8.78	-14.07	-6.57
	threshold	-1.67	-8.31	-5.86	-2.50	-8.85	-5.37
	cross-corr	-1.86	-8.00	-5.79	-2.97	-9.03	-5.67

From the result of experiment, it can be seen that each methods gives different TDOAs values that approaching the TDOAs ideal value. The following table show values of TDOAs mean from each methods for square array configuration, with noise source coordinate P1 = [-3.13, -9.21, 4.22] meter and P2 = [-7.36, -13.72, 0.84] meter.

From Fig. 11, we can get the frequency value of noise source. The value of this noise source frequency is 125 MHz. From Fig. 13, it can be seen that some points of estimated location in both noise source locations are far from the true location of noise source. It happened due to reflections from the objects in the surrounding environment, so that the received signal is the sum of noise source signal and reflected signals from the objects in the surrounding environment. Besides, the factor of TDOAs estimation method and the divergence from Newton-Raphson equation to get noise source location also affect the result of location estimation that far from the true location of noise source.

By comparing Table 2 and Table 3, the average difference between TDOAs ideal value and TDOAs value from experimental results is 0 – 0.02 nanosecond (for cross-correlation method).

To get the accuracy of location estimation, we can do the following steps:

1. Find the error value ( $\epsilon$ ) for each sampling, by using equation  $\epsilon = \frac{|r - r_{\text{true}}|}{r_{\text{true}}}$ .  $r_{\text{true}}$  is the distance from point of origin (0,0,1) to the true noise source location.
2. Add all the  $\epsilon$  value and divide it by the number of sampling (this is the mean of  $\epsilon$  value).

By entering the value of  $\epsilon$  mean that has been obtained to the efficiency formula ( $\eta = 1 - \epsilon$ ), we get the value of accuracy 70.25 %.

From the simulation and experimental result above, we can conclude that:

1. Generally, the longer the baseline length give the better location accuracy.
2. The simulation to detect noise source can be applied in low-noise environment fairly good, with the average difference between TDOAs ideal value and TDOAs value from experimental results is 0 – 0.02 nanosecond.
3. From the several methods used in simulation to get the TDOAs value, cross-correlation method have the highest accuracy 95.84% (for d = 4 m), with an error 0 - 0.58 meter.
4. The accuracy of location estimation will be better for detect noise source that parallel to the antenna height, because error value for z-axis coordinate is zero.

## REFERENCES

- [1] F. H. Kreuger, Discharge Detection in High Voltage Equipment. London: Temple Press, 1964, ch. U.K.
- [2] J. P. Steiner, P. H. Reynolds, and W. L. Weeks, "Estimating the location of partial discharges in cables," IEEE Trans. Electr. Insul., vol. 27, no. 1, pp. 44–59, Feb. 1992.
- [3] B. Quak, E. Gulski, F. J. Wester, and P. N. Seitz, "Advanced PD site location in distribution power cables," in Proc. 7th Int. Conf. Properties and Applications of Dielectric Materials, vol. 1, 2003, pp. 183–186.
- [4] M. S. Mashikian, "Preventive maintenance testing of shielded power cable systems," IEEE Trans. Ind. Appl., vol. 38, no. 3, pp. 736–743, May/Jun. 2002.
- [5] Knapp, C. H. and G. C. Carter, "The generalized correlation method for estimation of time delay," IEEE Trans. on Acoustic, Speech, Signal Processing, Vol. 24, No. 4, 320–327, 1976.
- [6] Challa, R. N. and S. Shamsunder, "Passive near-field localization of multiple non-Gaussian sources in 3-D using cumulates," Signal Proc., Vol. 65, 39–53, 1998.
- [7] Tungkanawanich, A., Z. Kawasaki, and K. Matsuura, "Analysis of VHF-wideband impulsive electromagnetic noises on power distribution lines," Trans. IEE Japan, Vol. 120-B, No. 11, 1538–1544, 2001.
- [8] R. Mardiana and Z. Kawasaki, "Broadband Radio Interferometer Utilizing a Sequential Triggering Technique for Locating Fast-Moving Electromagnetic Sources Emitted from Lightning," IEEE Transactions on Instrumentation and Measurement, vol. 49, No.2, April 2000.
- [9] M. S. Soliman, A. Hirata, T. Morimoto, and Z. Kawasaki, "Numerical and Experimental Study on Three-Dimension Localization for Ultra-Wideband Impulsive Noise Resources", J. of Electromagnetic Waves and Application, Vol. 19, No.2, 175-187, 2005.
- [10] M. S. Soliman, A. Hirata, T. Morimoto, and Z. Kawasaki, "Computational and Experimental Study on the Localization of Impulsive Noise Sources", International Union of Radio Science, XXVII<sup>th</sup> General Assembly, B8.P.7, 542, August 2002.
- [11] N. Oussalah, Y. Zebboudj, and S. A. Boggs, "Partial Discharge Pulse Propagation in Shielded Power Cable and Implications for Detection Sensitivity", IEEE Trans. Electr. Insul., vol. 23, no.6, pp. 5–10, Nov/Dec. 2007